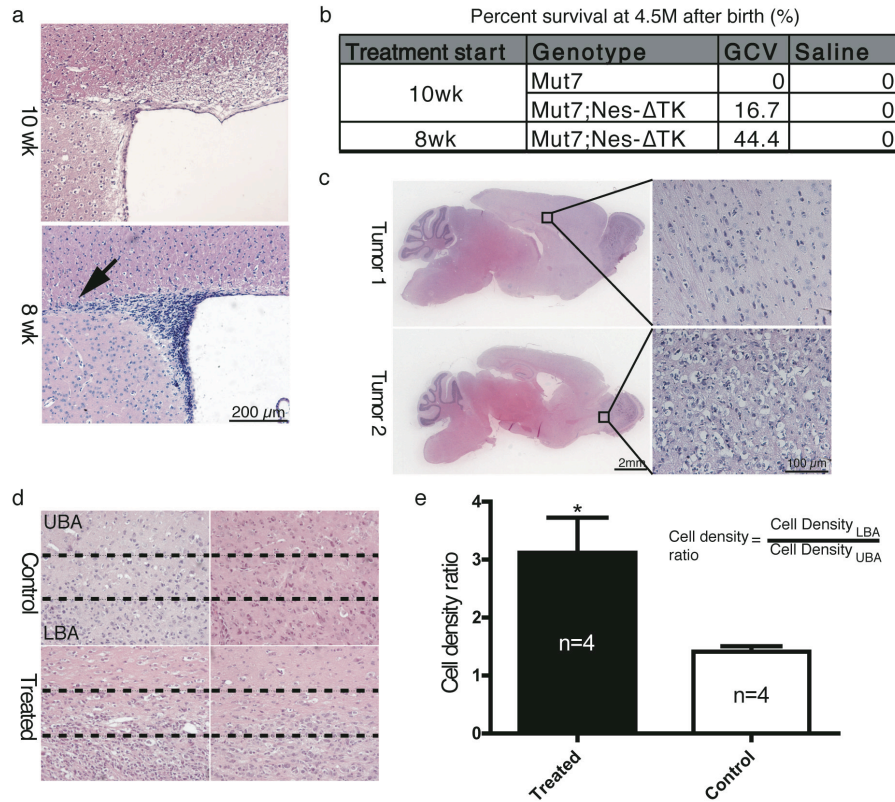
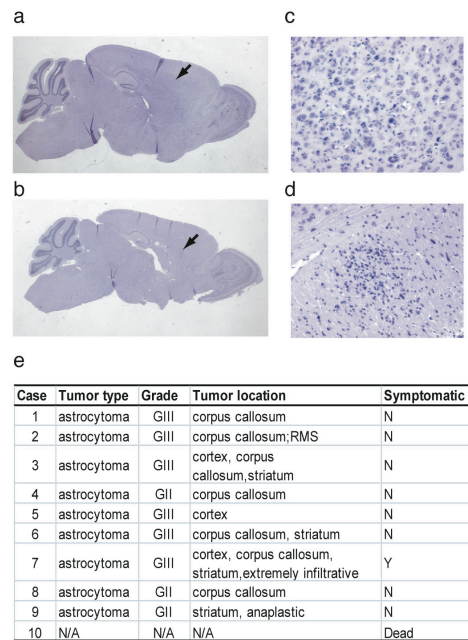


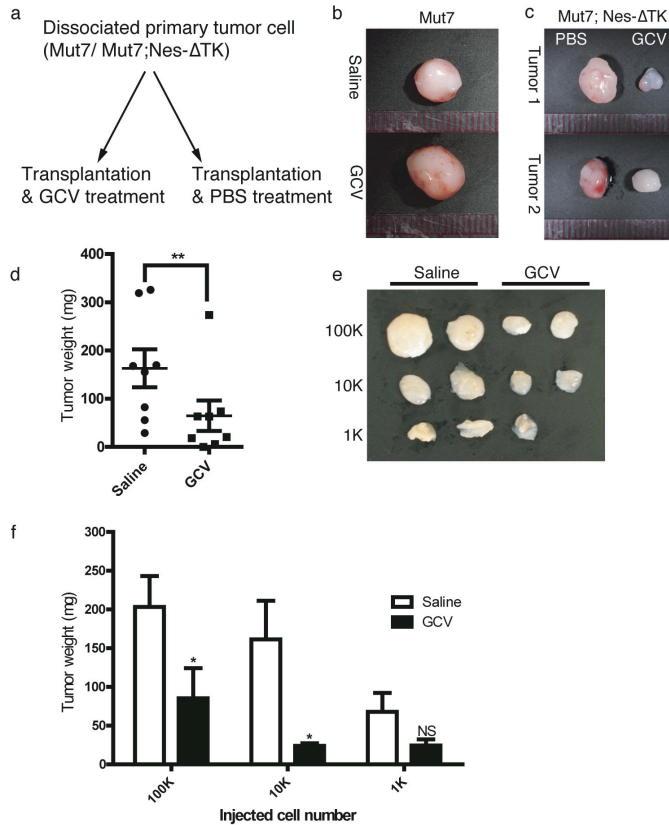
Supplementary Figure 1. *Nes-ΔTK-GFP*-expressing tumor cells can give rise to both GFP-positive and GFP-negative cells. **a**, Schema of temozolomide (TMZ) treatment and long-term labeling with BrdU analogs. *Mut7;Nes-ΔTK-GFP* mice were treated with TMZ for 5 days and injected with CldU for three days starting one day after the final TMZ treatment. IdU was injected seven days after the first CldU injection. **b**, GFP/CldU/IdU immunostaining of *Mut7;Nes-ΔTK* mice treated with TMZ and labeled with BrdU analogs. GFP-negative and CldU-positive cells are indicated by yellow arrowheads. CldU-positive cells that retain GFP expression are indicated by yellow arrows. **c**, IdU-incorporating cells (yellow arrows) are mostly derived from CldU-positive cells indicating that the emergent population of proliferating cells arose from *Nes-ΔTK-GFP*-expressing cells. **d**, Schema of glioma stem cell hierarchy and theoretical status of *Nes-ΔTK* transgene expression, GFP brightness, and proliferative potential. Note that these are not absolute transitions. We hypothesize that this is a gradual process such that some transient amplifying cells may still have the transgene on.



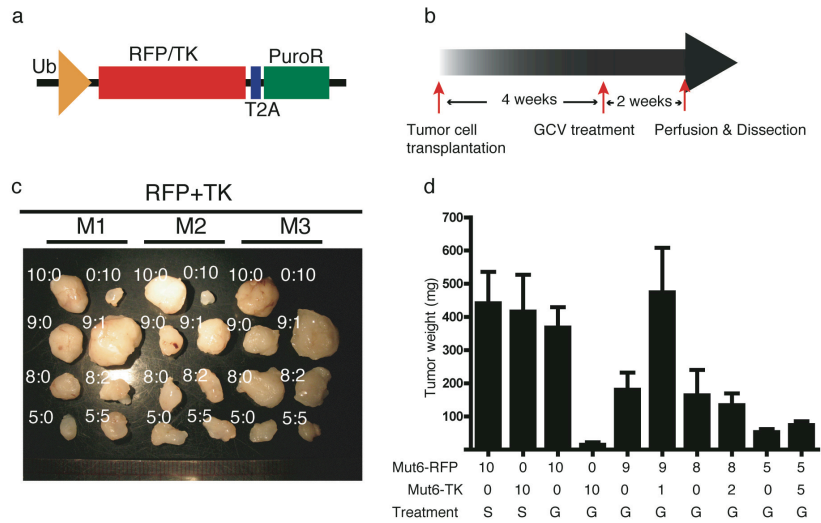
Supplementary Figure 2. Analysis of gliomas from GCV-treated *Mut7;Nes- $\Delta$ TK* mice. **a**, Representative H&E staining of *Mut7;Nes- $\Delta$ TK* SVZ treated with GCV from 10 or 8 weeks of age. Arrow indicates the rostral migratory stream, which was still present in some mice treated with GCV from 8 weeks of age due to inconsistent drug delivery caused by technical problems with the GCV minipump surgeries. **b**, Percentage of mice surviving at 4.5 months after birth following different treatment regimens. GCV-treatment of *Mut7;Nes- $\Delta$ TK* mice beginning at 8 weeks of age increased the 4.5 month survival rate to 44.4% compared to 0% with saline treatment. **c**, H&E staining of brain sections from two different *Mut7;Nes- $\Delta$ TK* mice treated with GCV from 8 weeks of age showing low grade lesions. **d,e**, GCV treatment reduced the infiltrative property of tumor cells in *Mut7;Nes- $\Delta$ TK* mice. **d**, Representative picture of the tumor edge area in saline- or GCV-treated gliomas from *Mut7;Nes- $\Delta$ TK* mice. The dashed lines divide each picture equally into 3 areas for quantification. The center of the tumors is located at the bottom in all figure panels. **e**, Quantification of tumor infiltration. The tumor cell density ratio was calculated as the density of the lower one-third boundary area (LBA) divided by the upper one-third boundary area (UBA). Data are mean  $\pm$  s.e.m.; \*,  $p < 0.05$ .



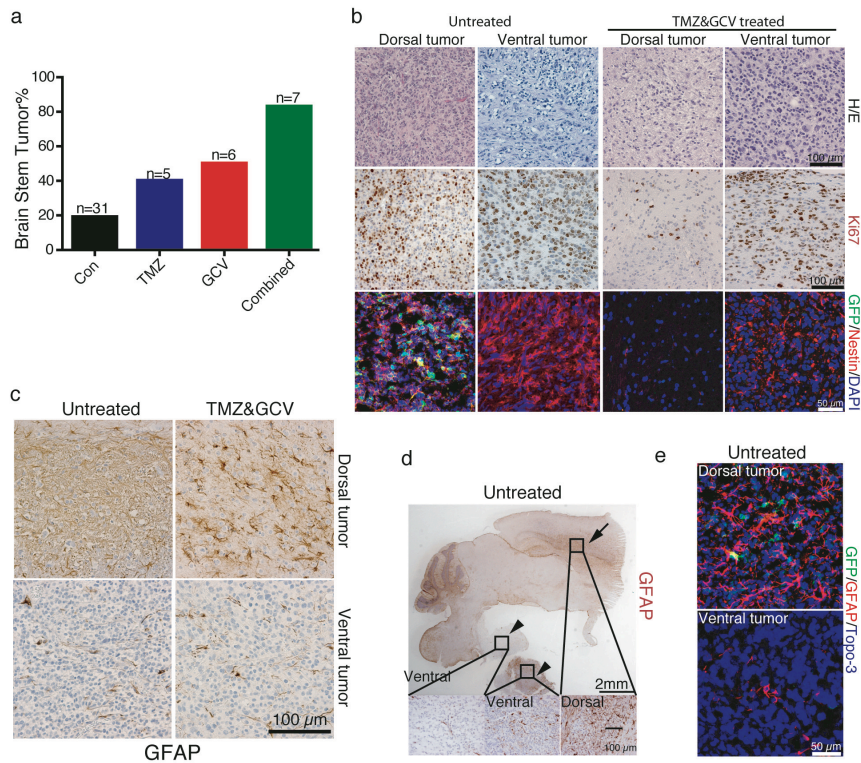
Supplementary Figure 3. Analysis of brain sections from 10-week-old untreated *Mut7* mice shows 100% incidence of astrocytomas. **a-d**, low magnification (**a,b**) and higher magnification (**c,d**) H&E staining of 10-week-old *Mut7* mouse brains with grade III (**a,c**) or grade II (**b,d**) glioma. Tumors are indicated by arrows. **e**, Summary of glioma types, grades and locations in brains of 10-week-old untreated *Mut7* mice. 9 out of 9 tumors were astrocytomas.



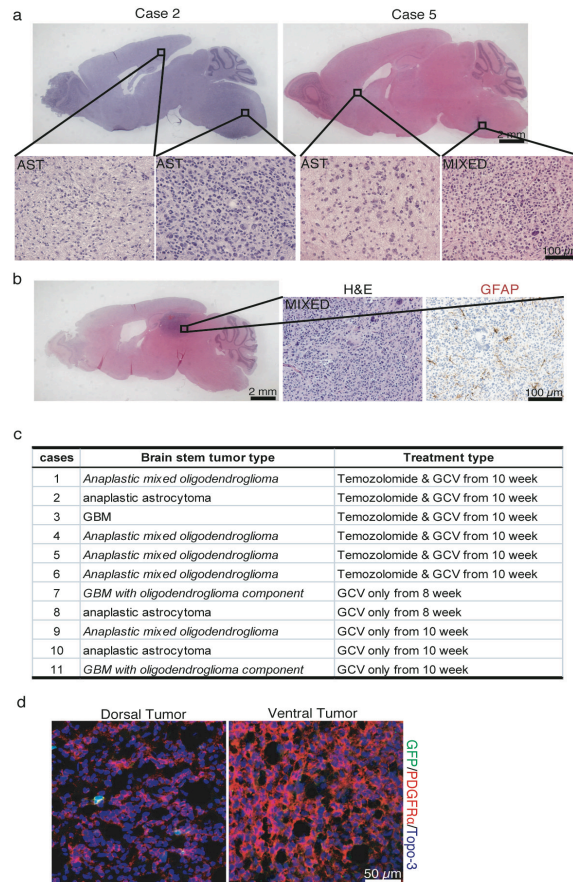
Supplementary Figure 4. *Nes-ATK*-positive cells are enriched for tumor-initiating and chemotherapy-resistant cells. **a**, Primary tumor transplantation schema. **b,c**, Representative tumor pictures from transplanted and GCV or PBS-treated *Mut7* (**b**) or *Mut7;Nes-ΔTK* (**c**) glioma. Tumors that developed from the GCV-treated host mice implanted with *Mut7;Nes-ΔTK* tumor cells were much smaller than those from the PBS- or GCV-treated host mice implanted with *Mut7* tumor cells or the PBS-treated host mice implanted with *Mut7;Nes-ΔTK* tumor cells. Ablation of GFP-positive cells slowed tumor growth in transplantation assays. **d**, Quantification of tumor weight 1 month after 100,000 primary tumor cells from *Mut7;Nes-ΔTK* mice were transplanted. \*\*,  $p < 0.01$ . **e**, Representative tumors and **f**, tumor weight quantification of allograft tumors 1 month after 100,000, 10,000 or 1,000 primary tumor cells from *Mut7;Nes-ΔTK* mice were transplanted. Glioma cells from 3 independent *Mut7;Nes-ΔTK* mice were used for the quantification. Data are mean  $\pm$  s.e.m.; \*,  $p < 0.05$ .



Supplementary Figure 5. The thymidine kinase (TK)-expressing cells did not induce an appreciable level of “bystander effect” in a transplantation assay. **a**, Schema of the lentiviral constructs used to overexpress TK or RFP. **b**, Experimental design schema for transplantation and GCV treatment to evaluate “bystander effect”. **c**, Picture of tumors after transplanting various combinations of RFP-expressing and TK-expressing GSCs, followed by GCV treatment. M1, M2, and M3 represent tumors harvested from 3 different nude mice. The ratio of RFP-expressing to TK-expressing cells ( $\times 10^4$ ) is shown in the picture. **d**, Quantification of tumor weights in (c); the ratio of RFP-expressing to TK-expressing cells ( $\times 10^4$ ) is presented on the x-axis. S and G correspond to saline and GCV treatment, respectively. Data are mean  $\pm$  s.e.m.



Supplementary Figure 6. Characterization of the GFAP-negative gliomas from *Mut7* or *Mut7;Nes-ΔTK* mice indicates they co-exist as separate tumors and do not arise from dorsal tumors following TMZ/GCV treatment. **a**, Percentage of brains with brain stem tumors in various treated groups. Control group includes treated or untreated *Mut7* mice and saline-treated *Mut7;Nes-ΔTK* mice. A much higher percentage of brain stem tumors was observed in the combinationally-treated *Mut7;Nes-ΔTK* mice. **b**, Representative H&E staining (top row), Ki67 immunostaining (middle row), and GFP/Nestin/DAPI staining (bottom row) of dorsal and ventral tumors in control and combinationally-treated *Mut7;Nes-ΔTK* mice. Ki67 staining indicates high proliferation in ventral tumors compared to the vestigial dorsal tumors. Note that the ventral tumors unmasked in the TMZ/GCV-treated mice are positive for endogenous nestin expression but negative for GFP expression. **c**, GFAP staining of cortex and brain stem tumors from untreated or TMZ/GCV-treated *Mut7;Nes-ΔTK* mice showed much lower level of GFAP expression in the ventral tumors. **d**, Representative GFAP immunostaining of *Mut7* tumor with both cortex (black arrows) and ventral (black arrowheads) tumors. Note the much higher level of GFAP staining in the dorsal tumor. **e**, GFP and GFAP double immunofluorescence staining of cortex and brain stem tumors from untreated *Mut7;Nes-ΔTK* mice. Very little GFAP expression and no GFP expression is observed in the ventral tumor.



Supplementary Figure 7. Ventral tumors with distinct histology emerge from TMZ/GCV-treated *Mut7;Nes-ΔTK* mice. **a**, Representative H&E staining of *Mut7;Nes-ΔTK* mice treated with temozolomide and GCV from 10 weeks of age. Higher magnification of pure astrocytic (AST, Case 2) and mixed oligodendrocytic (MIXED, Case 5) gliomas in the brain stem region. **b**, H&E and GFAP staining of the only midbrain tumor to arise in *Mut7;Nes-ΔTK* mice following combinational TMZ/GCV treatment. This tumor also showed oligodendroglioma features at higher magnification. **c**, Summary of brain stem tumor histology in treated *Mut7;Nes-ΔTK* mice. **d**, Representative GFP and PDGFR- $\alpha$  staining of cortical (dorsal) and brain stem (ventral) tumors. Note the ventral tumor has much higher levels of PDGFR $\alpha$  expression, a marker of oligodendroglioma.